Simulation of Analog Solution of Boolean Satisfiability

Technical Report UT-EECS-15-735

R. Joseph Connor
Jeremy Holleman
Bruce J. MacLennan
Jared M. Smith*

Department of Electrical Engineering and Computer Science
University of Tennessee
Knoxville, Tennessee 37996
Email: {rconnor6, jhollema, maclennan, jms}@utk.edu

September 28, 2015

Abstract

We present an analog implementation of a dynamical system for solving Boolean satisfiability, an NP-complete problem. Simulations of modest-sized hardware implementations in the presence of noise and integrator offset demonstrate that the algorithm is suitable for implementation in analog electronics.

1 Introduction

1.1 Boolean Satisfiability

The Boolean Satisfiability problem (SAT) is to find a set of 0/1 assignments to the Boolean variables $X_1, \ldots, X_n$ so that a specified Boolean expression is true (= 1). The Boolean expressions are in *conjunctive normal form*, e.g.:

$$(X_1 + X_3 + X_4) \cdot (\overline{X_2} + X_3 + X_4) \cdot (X_2 + X_4 + \overline{X_5}).$$

In this instance, there are $N = 5$ variables and $M = 3$ *clauses*. Positive or complemented variables (e.g., $X_2, \overline{X_2}$) are called *literals*. If every clause contains exactly k literals (as in the above example, $k = 3$), then it is an instance of the k-SAT problem. k-SAT is an NP-complete problem.

The difficulty of a particular instance is related to the *constraint density*, $\alpha = M/N$ [1].

1.2 ACTNN-k-SAT Algorithm

Ercsey-Ravasz and her colleagues present a continuous-time dynamical system for solving k-SAT [2, 3]. There are N bounded variables s_i which evolve to a solution, positive for Boolean 1, and negative for Boolean 0. In addition, there are M bounded variables a_m that measure the "urgency" of satisfying a clause. A particular problem instance is represented by an $M \times N$ constraint matrix $\mathbf{c}$, where $c_{mi} \in \{-1, 0, 1\}$. $c_{mi} = +1$ if X_i is positive in clause m, $c_{mi} = -1$ if $\overline{X_i}$ is in clause m, and $c_{mi} = 0$ if X_i does not occur in clause m.

The dynamical system is defined by the differential equations:

$$\dot{s}_i(t) = -s_i(t) + Af[s_i(t)] + \sum_{m=1}^{M} c_{mi} g[a_m(t)],$$

$$\dot{a}_m(t) = -a_m(t) + Bg[a_m(t)] - \sum_{i=1}^{N} c_{mi} f[s_i(t)] + 1 - k.$$

The *self-coupling parameters* A and B are two real constants that depend weakly on k. The f and g activation functions are piece-wise linear squashing functions that map the s and a values into $[-1, 1]$ and $[0, 1]$, respectively:

$$f(s) = (|s+1| - |s-1|)/2 = \begin{cases} -1 & \text{if } s < -1, \\ s & \text{if } -1 \le s \le 1, \\ +1 & \text{if } s > 1. \end{cases}$$

$$g(a) = (1 + |a| - |1-a|)/2 = \begin{cases} 0 & \text{if } a < 0, \\ \text{a} & \text{if } 0 \le a \le 1, \\ +1 & \text{if } a > 1. \end{cases}$$

Molnár and Ercsey-Ravasz [2] prove that the only stable fixed points of the system are solutions to the problem, and they give numerical evidence that there are no limit cycles, provided that the A and B parameters are in the appropriate range. Typical good ranges for the constants are $1 < A < 2$ and $2 < B < 2\lfloor k/2 \rfloor + 2$. If in fact there are no limit cycles in these ranges, then unsolvable instances would have chaotic attractors. This is consistent with the observed transient chaotic behavior for hard instances [2].

Molnár and Ercsey-Ravasz [2] prove the following bounds on the variables:

$$|s_i(t)| \leq 1 + A + \sum_m |c_{mi}|,$$
$$-2k \leq a_m(t) \leq 2 + B,$$

provided that they are initially in the ranges $|s_i(0)| \leq 1$ and $0 \leq a_m(0) \leq 1$. This guaranteed bounding of variables is critical for analog implementations, because variables in analog computational systems are bounded by their physical representation. The initial values are otherwise arbitrary.

The progess toward solution can be tracked by the following "energy function" which depends on the number of unsatisfied clauses [1, 2]:

$$E[f(\mathbf{s})] = \mathbf{K}^{\mathrm{T}}\mathbf{K} \text{ where } K_m = 2^{-k} \prod_{i=1}^{N} [1 - c_{mi} f(s_i)].$$

Note that E is not a Lyapunov function, and energy does not decrease monotonically.

1.3 Analog Implementation of ACTNN-k-SAT

Figure 1 displays an analog algorithm for implementing this dynamical system. The overall structure is a cross-bar between the M integrators for the a_m and the N integrators for the s_i; thus $M + N$ integrators are required. A particular instance is programmed by setting the c_{mi} and $-c_{mi}$ connections to $-1, 0$, or $+1$, as required for the problem. The integrators are initialized to small values to start the computation; non-zero offset or noise in the hardware integrators might have the same effect.

This structure is easily implemented in analog form, as it comprises a small number of simple components repeated in a regular pattern. Integrators are a ubiquitous element of analog signal processing systems, with numerous switched-capacitor[4][5], continuous-time voltage-mode, and current-mode implementations [6]. Clamping, scaling, and summation are likewise easily implemented, particularly using current-mode signaling. The weights $c_{m,i}$ can easily be implemented using cross-bar switches.

Analog computation has been demonstrated to provide outstanding energy efficienty at moderate resolutions, often yielding energy efficiency improvements of multiple orders of magnitude over digital implementations [7, 8]. However, with that efficiency comes imperfect computation, as every element injects error into a calculation. These errors can be reduced, but at the cost of increased silicon area and power

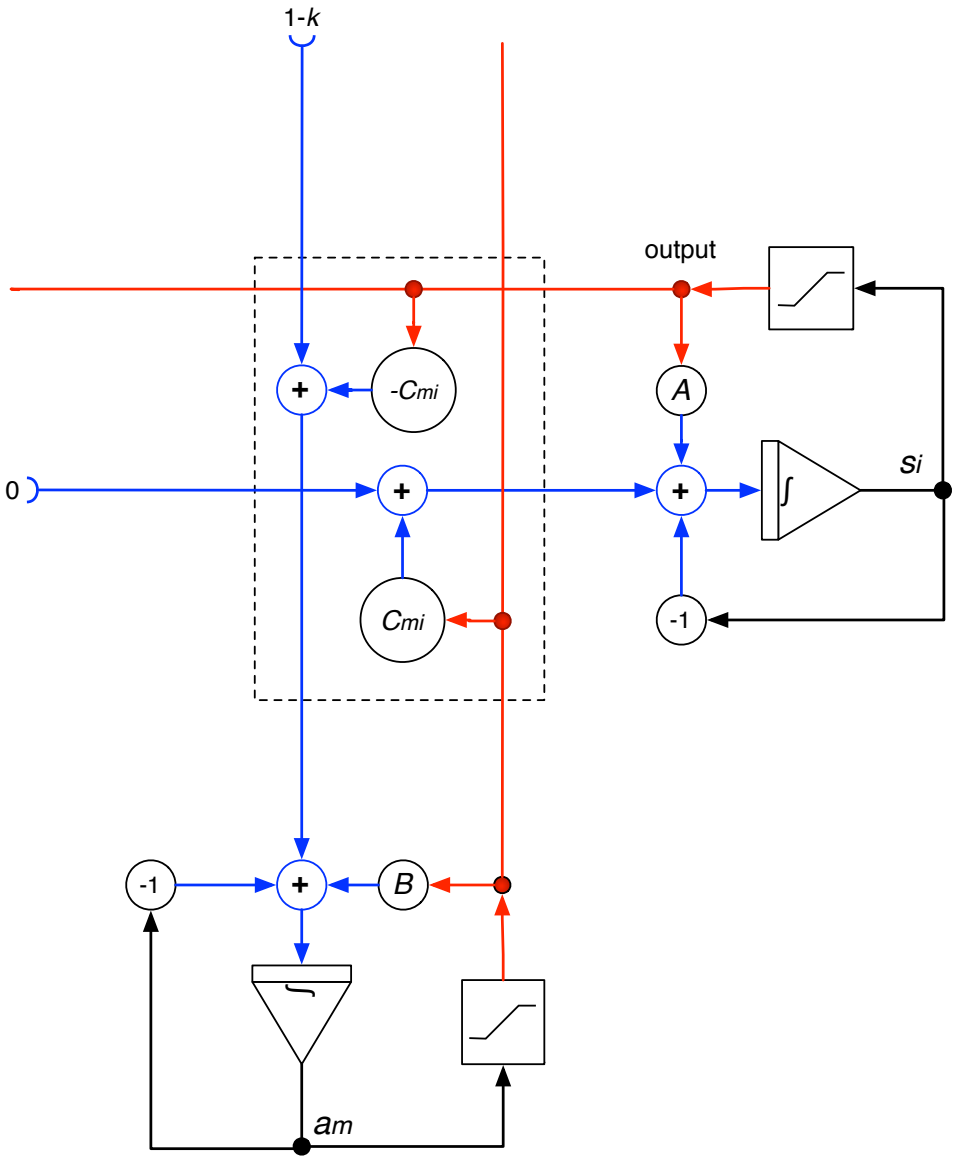

Figure 1: Analog Implementation of ACTNN-k-SAT.

consumption. In order to ensure that circuit performance does not degrade algorithmic performance, while avoiding excessive power and area due to over-engineering, designers must carefully model the effects of non-ideal computation. In this paper, we address that modeling task for the ACTNN-k-SAT solver, focusing primarily on noise and offsets.

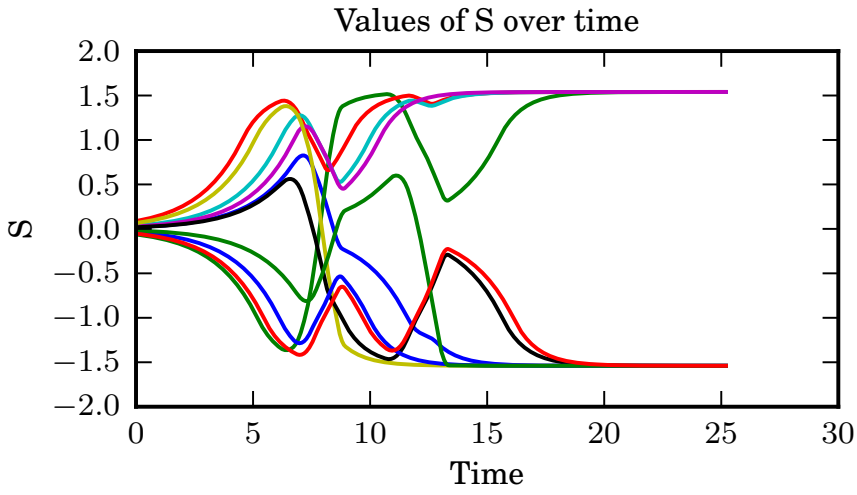

Figure 2: Evolution of s variables over time for a typical $\alpha = 4$ 4-SAT problem.

2 Simulation

Previous simulations have demonstrated that the algorithm is resilient in the face of significant noise in the interconnection weight c_{mi} and integrations [3]. In preparation for an eventual implementation in analog electronics, we developed a simple simulation program in order to evaluate performance of the algorithm. For the small instances of k-SAT that we have in mind ($N \approx 10, M < 50$) we use a simple forward-Euler method. We established that a time step $\Delta t = 0.02$ gives reliable results, and it was used in the simulations reported here. We focused on 4-SAT problems and used self-coupling parameters $A = 1.54$ and $B = 2.18$, which are in the optimal region established by Molnár and Ercsey-Ravasz [2]. Simulations were run for a maximum of $t_{\max} = 100$ time units, and were deemed to have failed to find a solution if unable to do so within this time.

Fig. 2 displays the evolution of the ten s variables over time for an example 4-SAT problem with a constraint density $\alpha = 4$. The graph show how some variables tentatively assume values early in the simulation, but change them later as the system is attracted to a solution state. Fig. 3 displays the evolution of the forty a variables for the same simulation. Careful comparison with Fig. 2 shows that increase in an a variable (corresponding to an unsatisfied constraint) leads to a sign change in an s variable. Finally, Fig. 4 shows the time evolution of the energy function, which reflects the urgency of satisfying unsatisfied constraints. A partial solution is found at $t \approx 8$ before a complete solution is discovered at $t \approx 18$.

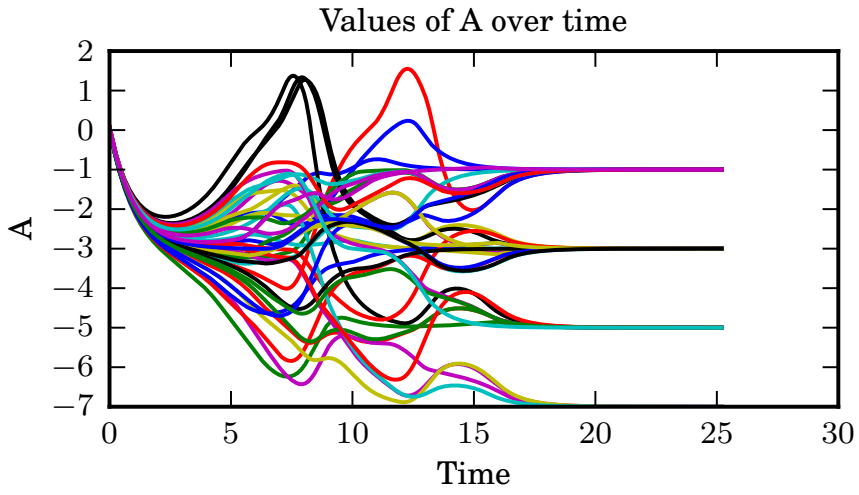

Figure 3: Evolution of a variables over time for a typical $\alpha = 4$ 4-SAT problem.

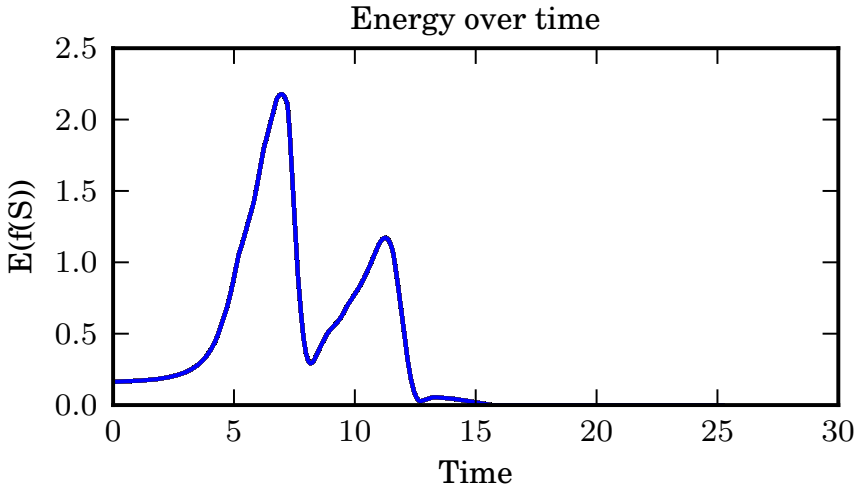

Figure 4: Evolution of E "energy" function over time for a typical $\alpha = 4$ 4-SAT problem.

3 Results

Fig. 5 displays the distribution of convergence times versus constraint density α for 100 randomly chosen constraint matrices for 4-SAT instances with no noise or offset. For $\alpha < 3.5$, all instances are solved in the allotted time, but for $\alpha \geq 3.5$ a few

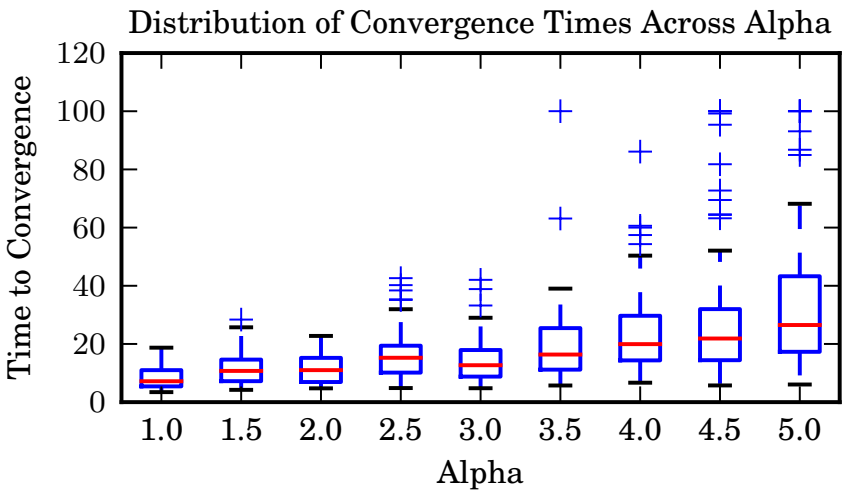

Figure 5: Distribution of convergence time versus difficulty measured by α for 100 random 4-SAT instances. ($t = 100$ represents non-convergence in the allotted time.)

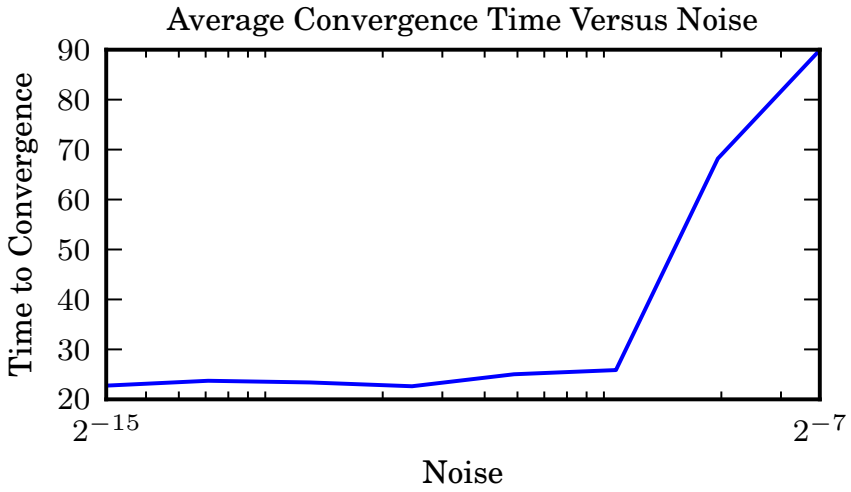

Figure 6: Convergence time versus noise for 100 random 4-SAT instances.

remained unsolved when the simulation was terminated. Therefore, in the following simulations we used $\alpha = 4.0$ to provide a baseline against which to compare the effects of noise and offset.

Fig. 6 displays the time to convergence for the same 100 random 4-SAT problems,

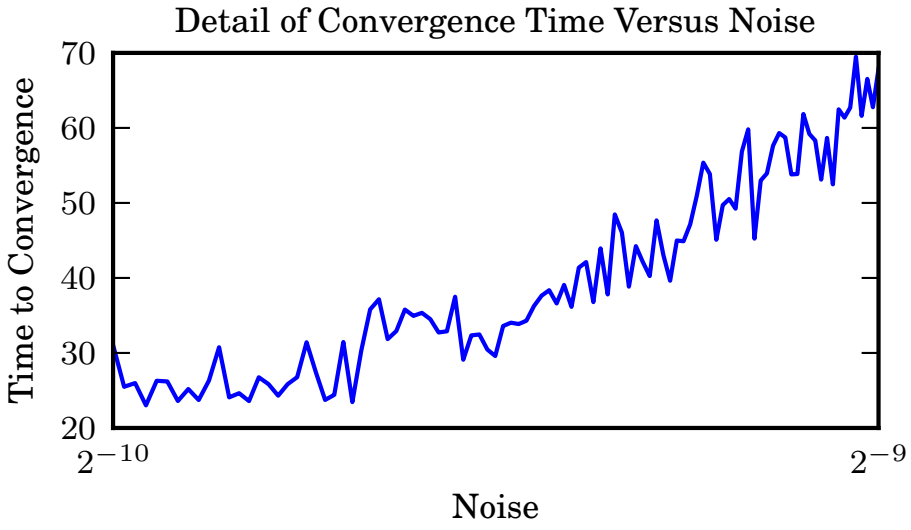

Figure 7: Detail of convergence time versus noise for 100 random 4-SAT instances, noise $\sigma = 2^{-10}$ to 2^{-9}.

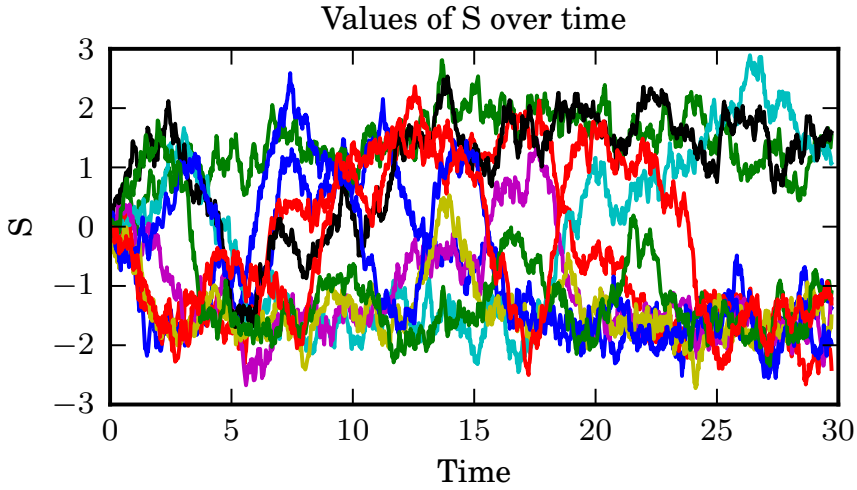

Figure 8: Effect of noise on evolution of s variables.

but with Gaussian noise σ varying from 2^{-15} to 2^{-7} of full range of the s and a variables. Noise had little effect on the system up through values of 2^{-10} (nearly 100% solved). At 2^{-9}, however, only about 40% of the problems were solved in the time set for the simulation. Additional noise levels were simulated in range of $2^{-10} - 2^{-9}$ where the critical transition seems to occur, as illustrated in Fig. 7

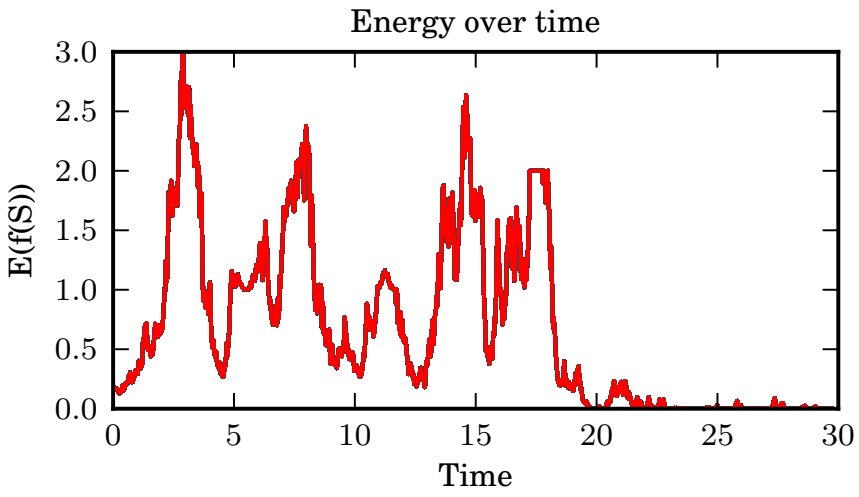

Figure 9: Effect of noise on evolution of energy.

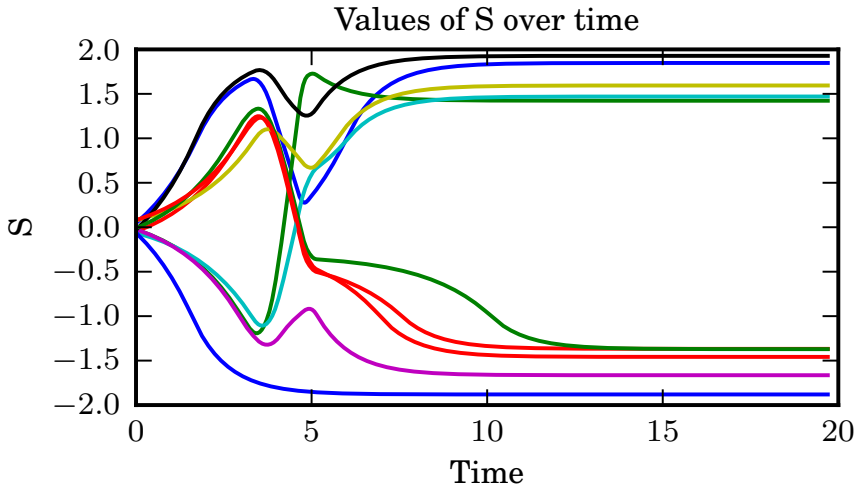

Figure 10: Effect of offset on evolution of s variables.

Figs. 8 and 9 show the effect of noise ($\sigma = 2^{-9}$ of full range of s and a variables) on the problem instance depicted in Figs. 2–4. Figs. 10 and 11 show the effect of offset ($\sigma = 2^{-13}$) on this same instance. The combined effects of noise and offset are shown in Figs. 12 and 13 ($\sigma = 2^{-10}$ noise and $\sigma = 2^{-12}$ offset). In all of these cases, despite the considerable noise in the s and a variables, the algorithm found a

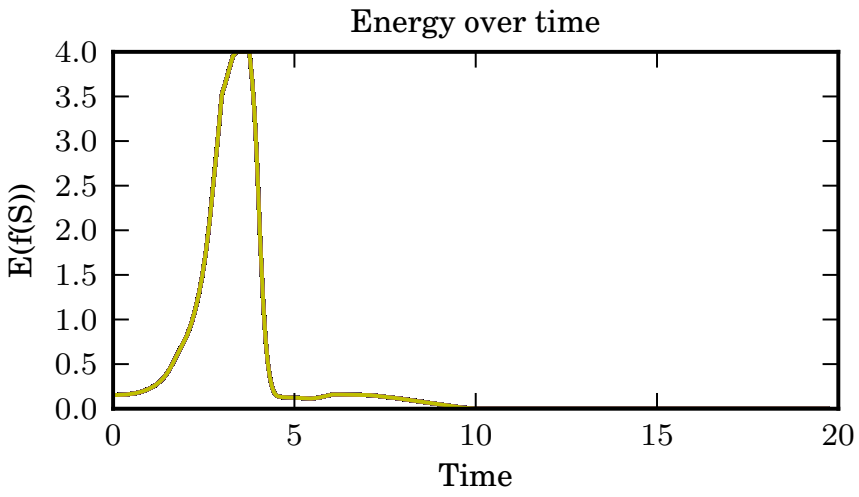

Figure 11: Effect of noise on evolution of energy.

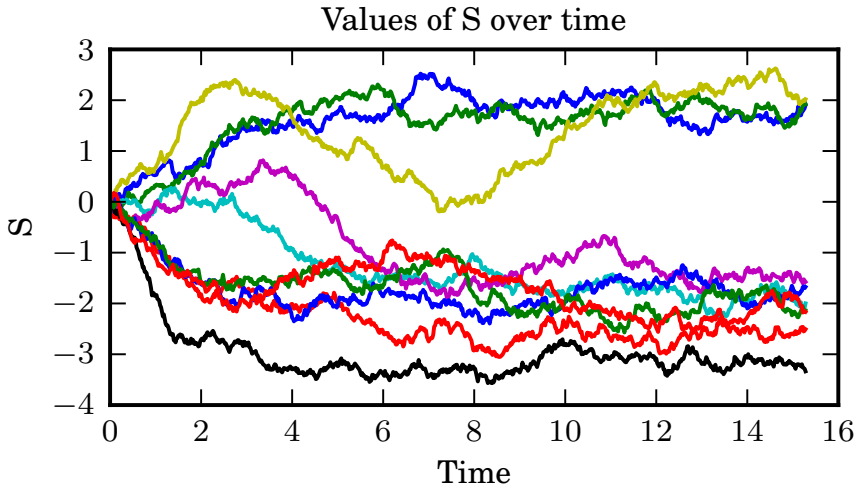

Figure 12: Combined effects of noise and offset on evolution of s variables.

solution in about the same time as the error-free version.

The effects of noise and offset on convergence are summarized in Fig. 14, which displays the percentage of this random selection of $\alpha = 4$ problems that were solved within the allotted time for a variety of combinations of noise and offset.

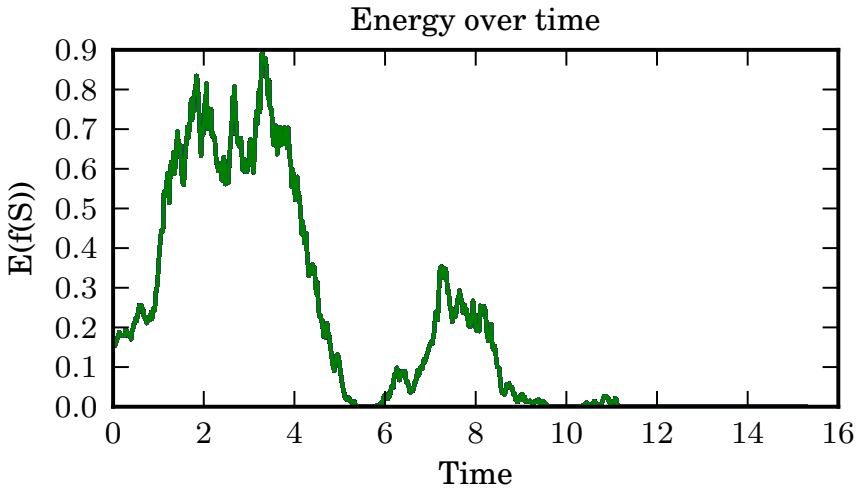

Figure 13: Combined effects of noise and offset on evolution of energy.

4 Conclusion

We have determined that this analog algorithm for Boolean satisfiability can solve modest-sized instances ($N = 10, \alpha = 4$) in the presence of moderate noise and offset error, and is thus suitable for implementation in analog electronics. Further study is required to determine whether the noise requirement can be relaxed further with longer running time. More relaxed noise budgets could allow faster and more efficient implementations, reducing the scaling factor relating the arbitrary time units used in these simulations to real-world time. Therefore even though solution times might increase in simulation with noisier circuits, the real-world solution time could decrease.

References

[1] M. Ercsey-Ravasz and Z. Toroczkai, "Optimization hardness as transient chaos in an analog approach to constraint satisfaction," *Nature Physics*, vol. 7, pp. 966–970, 2011.

[2] B. Molnár and M. Ercsey-Ravasz, "Asymmetric continuous-time neural networks without local traps for solving constraint satisfaction problems," *PLoS ONE*, vol. 8, no. 9, p. e73400, 2013.

[3] R. Sumi, B. Molnár, and M. Ercsey-Ravasz, "Robust optimization with transiently chaotic dynamical systems," *EPL (Europhysics Letters)*, vol. 106, p. 40002, 2014.

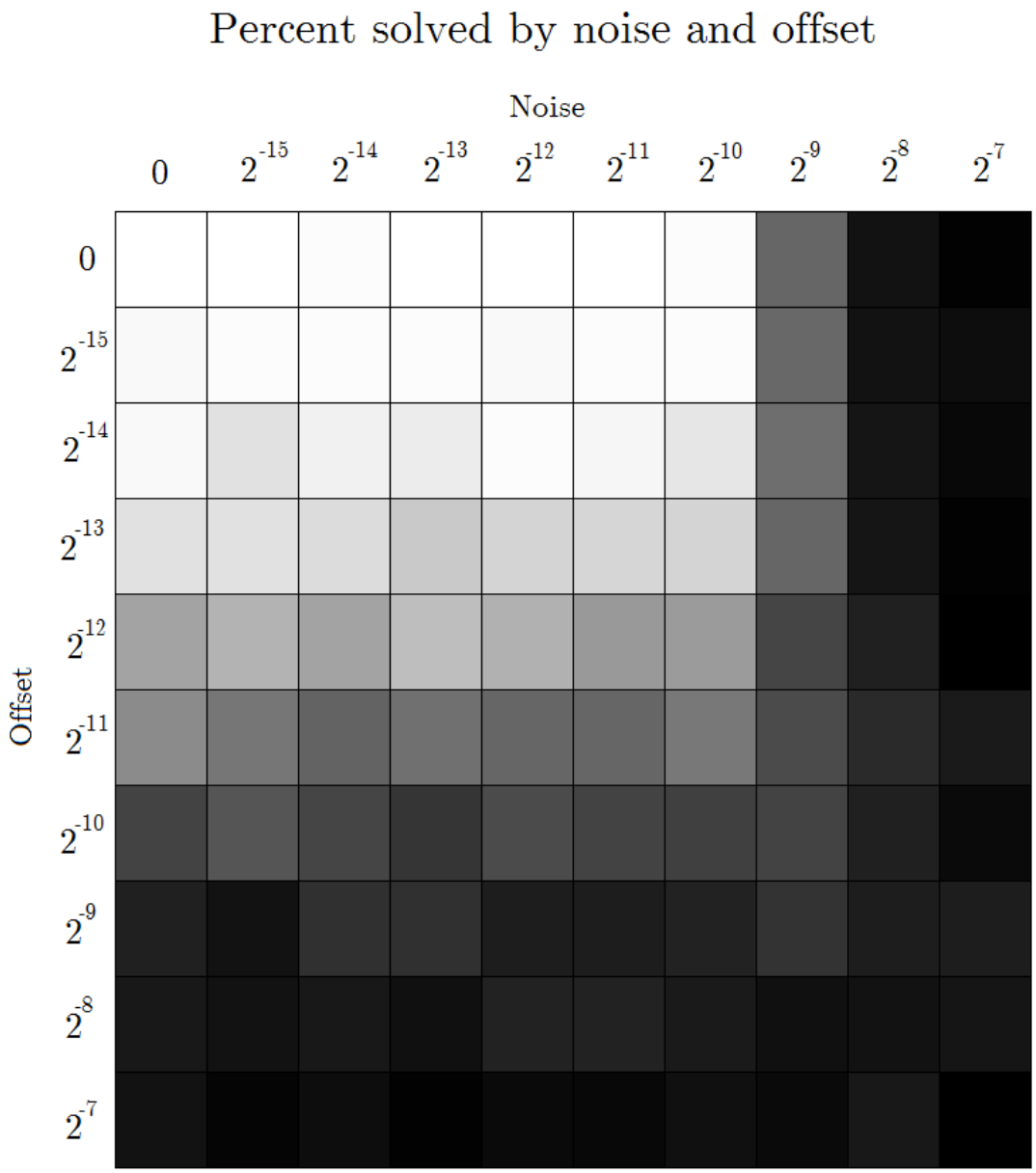

Figure 14: Percent of $\alpha = 4$ problems solved for various combinations of noise and offset. Key: white = 100%, black = 0%.

[4] Y. Zhang, C.-H. Chen, and G. Temes, "Accuracy-enhanced switched-capacitor stages using low-gain opamps," *Electronics Letters*, vol. 49, no. 1, pp. 22–23, 2013.

[5] D. J. Allstot, R. W. Brodersen, and P. R. Gray, "Mos switched capacitor ladder filters," *Solid-State Circuits, IEEE Journal of*, vol. 13, no. 6, pp. 806–814, 1978.

[6] W. A. Serdijn, M. Broest, J. Mulder, A. C. van der Woerd, and A. H. van Roermund, "A low-voltage ultra-low-power translinear integrator for audio filter applications," *Solid-State Circuits, IEEE Journal of*, vol. 32, no. 4, pp. 577–581, 1997.

[7] J. Lu and J. Holleman, "A 1 TOPS/W analog deep machine-learning engine with floating-gate storage in 0.13 *upmu* m CMOS," in *IEEE International Solid-State Circuits Conference Digest of Technical Papers*, February 2014.

[8] R. Chawla, A. Bandyopadhyay, V. Srinivasan, and P. Hasler, "A 531 nw/mhz, 128× 32 current-mode programmable analog vector-matrix multiplier with over two decades of linearity," in *Custom Integrated Circuits Conference, 2004. Proceedings of the IEEE 2004*. IEEE, 2004, pp. 651–654.